Organic photovoltaic cells based on an acceptor of soluble graphene

Qian Liu,[1] Zunfeng Liu,[2] Xiaoyan Zhang,[2] Nan Zhang,[1] Liying Yang,[1] Shougen Yin,[1,a)] and Yongsheng Chen[2,a)]
[1]*Key Laboratory of Display Materials and Photoelectric Devices (Tianjin University of Technology), Ministry of Education, Institute of Material Physics, Tianjin University of Technology, Tianjin 300384, People's Republic of China*
[2]*Key Laboratory for Functional Polymer Materials and Center for Nanoscale Science and Technology, Institute of Polymer Chemistry, College of Chemistry, Nankai University, Tianjin 300071, People's Republic of China*

(Received 2 February 2008; accepted 7 May 2008; published online 2 June 2008)

In this paper, an organic photovoltaic device based on an acceptor of solution-processable functionalized graphene was designed. A short circuit current density (J_{sc}) of 4.0 mA cm^{-2}, open circuit voltage (V_{oc}) of 0.72 V, and a solar power conversion efficiency of 1.1% were obtained for the device of indium tin oxide/poly(ethylene dioxythiophene) doped with polystyrene sulfonic acid (40 nm)/poly(3-hexylthiophene-1, 3-diyl):graphene (graphene 10 wt %, 100 nm)/LiF (1 nm)/Al (70 nm) after an annealing treatment under simulated AM1.5G 100 mW illumination in air. Because of the low price, ease of preparation, and inertness against ambient conditions, soluble graphene will be a promising candidate used for acceptor materials in the photovoltaic applications. © *2008 American Institute of Physics*. [DOI: 10.1063/1.2938865]

Graphene, the only two dimensional crystal of sp^2 hybridized carbon, has attracted much attention since it was experimentally demonstrated that the material is stable at ambient conditions.[1] Electrons in graphene obey a linear dispersion relation and behave like massless relativistic particles,[2] resulting in the observation of a number of very peculiar electronic properties such as the quantum Hall effect,[3–6] ambipolar electric field effect,[1] and transport via relativistic Dirac fermions.[7,8] The graphene layer displays high electron mobility, long phase coherence and elastic scattering lengths, and quantum confinement effects.[9] Based on its fundamental electronic properties and semimetallic nature, graphene has been used to fabricate a number of simple electronic devices such as field-effect transistors,[10–14] resonators,[15] and quantum dots.[16] Thin films obtained from graphene have also been used as transparent electrodes in device applications due to their high conductivity, excellent transparency, high chemical, and thermal stabilities.[17,18]

In this paper, graphene was used as the acceptor material in the bulk heterojunction (BHJ) organic photovoltaic cells. To achieve good dispersion of graphene in conjugated polymer, a solution-processable functionalized graphene (SPFGraphene) was used in this paper, which is prepared by a two step method: an oxidation step, then an organic functionalization step.[19] The oxidation treatment using a modified hummers method[20,21] of the flake graphite gave out graphene oxide sheets having a thickness of ~0.7 nm and a dimension of several hundred nanometers, as shown in Fig. 1(c). Then a phenyl isocyanate treatment[19] gave out SPFGraphene which can be dissolved in organic solvent such as 1,2-dichlorobenzene (DCB). The photovoltaic device was made using a common fabrication process. The active layer was prepared by spin coating a poly(3-hexylthiophene-1,3-diyl) (P3HT), (15 mg ml^{-1})/SPFGraphene solution in DCB (SPFGraphene content: 0%, 2.5%, 5%, 10%, and 15%) onto an indium tin oxide (ITO) glass substrate which is precoated with poly(ethylene dioxythiophene) doped with polystyrene sulfonic acid (PEDOT: PSS, a conducting polymer). Then LiF and Al were vapor deposited on the active layer. The chemical structures of graphene and P3HT are shown in Fig. 1(a). The schematic representation of the P3HT/graphene based solar cell is shown in Fig. 1(b), which has a structure of ITO (~17 Ω sq^{-1})/PEDOT:PSS (40 nm)/P3HT:graphene (100 nm)/LiF (1 nm)/Al (70 nm). The effective area of each cell is ~8 mm^2. The current-voltage (J-V) curves of the photovoltaic devices are determined using an AM1.5G standard operating with an illumination intensity of 100 mW cm^{-2}, as shown in Fig. 2. (Also see Ref. 22 for experimental details.)

Figure 2(a) shows the current density (J)-voltage (V) curves of the photovoltaic devices based on P3HT and P3HT/graphene in dark and under illumination without annealing treatment. It can be seen that there is no current response in dark for the two photovoltaic devices, the high dark current under forward bias indicates distinct diode behavior. Under illumination, the device based on pristine P3HT gives power conversion efficiency (η) of 0.005%, short circuit current density (J_{sc}) of 0.04 mA cm^{-2}, and open

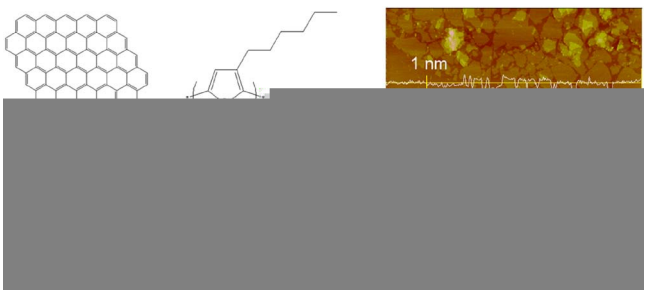

FIG. 1. (Color online) (a) The chemical structures of graphene and P3HT are shown in the up panel. (b) Schematic of the devices with P3HT/graphene thin film as the active layer is shown in the middle panel, ITO (~17 Ω sq^{-1})/PEDOT:PSS (40 nm)/P3HT:graphene (100 nm)/LiF (1 nm)/Al (70 nm). (c) Atomic force microscopy picture of the graphene oxide in a tapping mode is shown in the right panel.

a)Authors to whom correspondence should be addressed. Electronic addresses: sgyin@tjut.edu.cn and yschen99@nankai.edu.cn. FAX: +86(22)-6021-5796. Tel.: +86(22)-6021-5558.

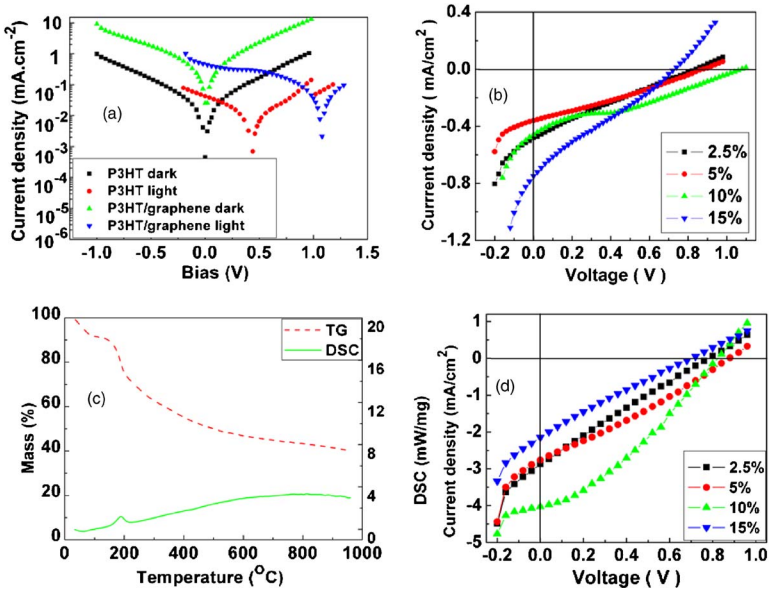

FIG. 2. (Color online) (a) Logarithmic *J-V* characteristics of the photovoltaic devices based on P3HT and P3HT/graphene in dark and under a simulated AM1.5G 100 mW illumination without annealing. (b) *J-V* characteristics of P3HT/graphene based photovoltaic devices of different graphene content (2.5%, 5%, 10%, and 15%) under a simulated AM1.5G 100 mW illumination without annealing. (c) TGA and DSC curve of the graphene during the range from 35 to 960 °C at a heating rate of 5 °C min^{-1} in Ar flow. (d) *J-V* characteristics of P3HT/graphene based photovoltaic devices of different graphene content (2.5%, 5%, 10%, and 15%) after annealing at 160 °C for 10 min under a simulated AM1.5G 100 mW illumination.

circuit voltage of (V_{oc}) of 0.42 V, while the P3HT/graphene based one gives η value of 0.15%, J_{sc} of 0.46 mA cm^{-2}, and V_{oc} of 1.1 V. The overall performance of P3HT/graphene based device is much higher than that of the control device based on pristine P3HT. Obviously, the improvement in the overall photovoltaic performance can be attributed to the addition of graphene. We then investigated the photovoltaic characteristics based on P3HT/graphene composite containing different graphene content (2.5%, 5%, 10%, and 15%), as shown in Fig. 2(b), and the performance details are listed in Table I. The devices having graphene content of 2.5%, 5%, 10%, and 15% show η values of 0.09%, 0.1%, 0.15%, and 0.13%, respectively, with V_{oc} values in the range of 0.7–1.1 V. It can be seen that with the increase in the graphene content, the overall performance increases first, reaching a peak power efficiency of 0.15% for 10% graphene content, and then decreases. The fill factors of most devices are only in the range of 0.2–0.3, which shows a high series resistance. We consider that the high series resistance should come from inefficient stacking morphology of graphene sheets and chemical modification may also destroy the π-conjugation of the graphene sheet and then result in a decrease in charge carrier mobility.

Compared to the control device based on pristine P3HT, the P3HT/graphene based one shows much higher V_{oc} values (from ~0.4 to ~0.7–1.1 V). There are different models describing the origin of V_{oc} in organic photovoltaic devices.[23–25] In a single layered organic photovoltaic cell in which the active layer is composed of a pure conjugated polymer, the V_{oc} is principally determined by the work function difference between the two metal electrodes, i.e., the metal-insulator-metal (MIM) model.[25] In this paper, the device based on pristine P3HT gives a V_{oc} value of 0.42 V, which well matches the work function difference between ITO anode (4.7 eV) and Al cathode (4.3 eV). In the solar cells having a BHJ structure, the MIM model is not applicable, and a Fermi level pinning[26] mechanism between the negative electrode and the acceptor material [such as C_{60} and single-walled nanotubes (SWNTs)] was applied to address the origin of V_{oc},[23,24] i.e., the upper limit of the V_{oc} is governed by the difference between the lowest unoccupied molecular orbital of C_{60} (Ref. 23) or the work function of SWNTs (Ref. 24) and the highest occupied molecular orbital level of the conjugated polymer. Furthermore, it can be influenced by some factors such as the feed ratio of the donor and the acceptor, processing conditions, etc.[27,28] Therefore, similar to the C_{60} and SWNTs based BHJ photovoltaic devices, the V_{oc} value of P3HT/graphene based one may be governed by the work function difference between graphene (4.5 eV) (Ref. 29) and P3HT (5.2 eV),[30] which is ~0.7 V. The V_{oc} values of the P3HT/graphene based devices in this paper are in the range of 0.7–1.1 eV, a little higher than the predicted one. This may be caused by the following reasons:

TABLE I. Performance details (V_{oc}, J_{sc}, FF, and η) of the photovoltaic devices having a structure of ITO (~17 Ω sq^{-1})/PEDOT:PSS (40 nm)/P3HT:graphene (100 nm)/LiF (1 nm)/Al (70 nm) before and after annealing at 160 °C for 10 min under a simulated AM1.5G 100 mW illumination.

Graphene content	Annealing	V_{oc} (V)	J_{sc} (mA cm^{-2})	FF	η (%)
0%	No	0.42	0.04	0.27	0.005
2.5%	No	0.84	0.48	0.23	0.09
5%	No	0.88	0.36	0.28	0.1
10%	No	1.1	0.46	0.3	0.15
15%	No	0.72	0.75	0.25	0.13
2.5%	Yes	0.78	2.9	0.24	0.55
5%	Yes	0.86	2.7	0.3	0.69
10%	Yes	0.72	4.0	0.38	1.1
15%	Yes	0.78	2.1	0.21	0.35

(1) Different from the pristine graphene sheet, the functionalized one was introduced by some functional groups and its large π-conjugated structure was partly isolated by the functional groups, which will alter the work function of graphene sheet more or less. (2) Like the case of SWNTs, the strong π-π conjugation between graphene and P3HT may shift up the Fermi level of graphene.[31]

After functionalization, the graphene sheet was introduced by many functional groups and π-conjugated structure was partly isolated by the functional groups. Therefore, the conductivity and electron mobility of the graphene sheet can be greatly decreased. This will limit the performance of the above P3HT/graphene based device. In view that the functional groups can be removed from the graphene sheet in an elevated temperature under an inert atmosphere, and the conductivity of the graphene sheet can be recovered,[17] then we investigated the thermal properties and the weight loss properties of the graphene using thermogravimetric analysis (TGA) and differential scanning calorimetry (DSC) under Ar atmosphere, as shown in Fig. 2(c). It can be seen that a great weight loss of 20% occurred from 150 to 250 °C and, at this temperature range, an obvious exothermic peak can be observed on the DSC curve. The weight loss at this temperature range can be attributed to the removal of functional groups from the graphene sheets. Thus, we expect the annealing treatment will improve the performance of the P3HT/graphene devices.

The *J*-*V* curves of the P3HT/graphene devices at 160 °C treatment for 10 min are shown in Fig. 2(d). The detailed photovoltaic characteristics are also listed in Table I. It can be seen that after annealing, there are great improvements in photovoltaic performance for all the devices. The η values are 0.55%, 0.69%, 1.1%, and 0.35% for the devices with graphene content of 2.5%, 5%, 10%, and 15%, respectively. After the annealing treatment, the cell efficiency also shows similar graphene content dependence as that without an annealing treatment. The cell performance increases first with the increase in graphene content, achieving a peak value of 1.1% at graphene content of 10%, and then decreases. The V_{oc} values are in the range of 0.7–0.9 V, slightly different from that of the unannealed ones, which may be attributed to work function change in graphene, resulting from the removal of the organic functional groups. A very interesting thing is that J_{sc} values increase by almost one order of magnitude and the fill factor also increases. Obviously, annealing process plays an important role in the improvement of device performance. With the removal of the functional groups and the recovery of the π-conjugated areas, the conductivity of the graphene sheet increase and the charge carrier transport mobility is greatly increased.[17] In addition, the morphology change in P3HT can also be an important contribution to the improvement in the device performance.[32]

In this paper, one atom thick carbon material, graphene, was used as the acceptor material in the organic photovoltaic cells. The graphene was chemically functionalized to be soluble, mixed with P3HT, and used as the active layer. After an annealing process, we get a performance of 1.1% for the device containing 10% graphene in the active layer. Besides the one-atom-thick plane structure feature, high hole transport mobility, large specific area, and the inertness against oxygen and water vapor of graphene make this material a promising candidate in photovoltaic applications.

The authors gratefully acknowledge the financial support from NSF (60676051, 20644004, 07JCYBJC03000) of China, Tianjin Natural Science Foundation (06TXTJJC14603), MoST (2006CB0N0702), MoE (20040055020), and Tianjin Key Laboratory for Photoelectric Materials and Devices.

[1] K. S. Novoselov, A. K. Geim, S. V. Morozov, D. Jiang, Y. Zhang, S. V. Dubonos, I. V. Grigorieva, and A. A. Firsov, Science **306**, 666 (2004).
[2] M. I. Katsnelson, Mater. Today **10**, 20 (2007).
[3] V. P. Gusynin1 and S. G. Sharapov, Phys. Rev. Lett. **95**, 146801 (2005).
[4] K. S. Nonoselov, E. McCann, S. V. Morozov, V. I. Fal'ko, M. I. Katsnelson, U. Zeitler, D. Jiang, F. Schedin, and A. K. Geim, Nat. Phys. **2**, 177 (2006).
[5] K. S. Novoselov, Z. Jiang, Y. Zhang, S. V. Morozov, H. L. Stormer, U. Zeitler, J. C. Maan, G. S. Boebinger, P. Kim, and A. K. Geim, Science **315**, 1379 (2007).
[6] Y. Zhang, Y. W. Tan, and P. Kim, Nature (London) **438**, 201 (2005).
[7] K. S. Novoselov, A. K. Geim, S. V. Morozov, D. Jiang, M. I. Katsnelson, I. V. Grigorieva, S. V. Dubonos, and A. A. Firsov, Nature (London) **438**, 197 (2005).
[8] S. Y. Zhou, G. H. Gweon, J. Graf, A. V. Fedorov, C. D. Spataru, R. D. Diehl, Y. Kopelevich, D. H. Lee, S. G. Louie, and A. Lanzara, Nat. Phys. **2**, 595 (2006).
[9] C. Berger, Z. Song, X. Li, X. Wu, N. Brown, C. Naud, D. Mayou, and T. L. Joanna, Science **312**, 1191 (2006).
[10] S. Gilje, S. Han, M. Wang, K. L. Wang, and R. B. Kaner, Nano Lett. **7**, 3394 (2007).
[11] D. Gunlycke, D. A. Areshkin, and C. T. White, Appl. Phys. Lett. **90**, 142104 (2007).
[12] M. Y. Han, B. Ozyilmaz, Y. Zhang, and P. Kim, Phys. Rev. Lett. **98**, 206805 (2007).
[13] B. Obradovic, R. Kotlyar, F. Heinz, P. Matagne, T. Rakshit, M. D. Giles, M. A. Stettler, and D. E. Nikonov, Appl. Phys. Lett. **88**, 142102 (2006).
[14] Y. Ouyang, Y. Yoon, J. K. Fodor, and J. Guo, Appl. Phys. Lett. **89**, 203107 (2006).
[15] J. S. Bunch, A. M. van der Zande, S. S. Verbridge, I. W. Frank, D. M. Tanenbaum, J. M. Parpia, H. G. Craighead, and P. L. McEuen, Science **315**, 490 (2007).
[16] B. Trauzettel, D. V. Bulaev, D. Loss, and G. Burkard, Nat. Phys. **3**, 192 (2007).
[17] X. Wang, L. Zhi, and K. Mullen, Nano Lett. **8**, 323 (2008).
[18] J. Wu, W. Pisula, and K. Mullen, Chem. Rev. (Washington, D.C.) **107**, 718 (2007).
[19] S. Stankovich, D. A. Dikin, G. H. B. Dommett, K. M. Kohlhaas, E. J. Zimney, E. A. Stach, R. D. Piner, S. B. T. Nguyen, and R. S. Ruoff, Nature (London) **442**, 282 (2006).
[20] W. Hummers and R. Offeman, J. Am. Chem. Soc. **80**, 1339 (1958).
[21] M. Hirata, T. Gotou, S. Horiuchi, M. Fujiwara, and M. Ohba, Carbon **42**, 2929 (2004).
[22] See EPAPS Document No. E-APPLAB-92-098822 for experimental details. For more information on EPAPS, see http://www.aip.org/pubservs/epaps.html.
[23] C. J. Brabec, A. Cravino, D. Meissner, N. S. Sariciftci, T. Fromherz, M. T. Rispens, L. Sanchez, and J. C. Hummelen, Adv. Funct. Mater. **11**, 374 (2001).
[24] E. Kymakis, I. Alexandrou, and G. A. J. Amaratunga, J. Appl. Phys. **93**, 1764 (2003).
[25] I. D. Parker, J. Appl. Phys. **75**, 1656 (1993).
[26] K. Yoshino, M. Onoda, Y. Manda, and M. Yokoyama, Jpn. J. Appl. Phys., Part 2 **27**, L1606 (1988).
[27] M. Al-Ibrahim, O. Ambacher, S. Sensfuss, and G. Gobsch, Appl. Phys. Lett. **86**, 201120 (2005).
[28] J. Liu, Y. Shi, and Y. Yang, Adv. Funct. Mater. **11**, 420 (2001).
[29] J. W. G. Wildoer, L. C. Venema, A. G. Rinzler, R. E. Smalley, and C. Dekker, Nature (London) **391**, 59 (1998).
[30] P. Andersson, N. D. Robinson, and M. Berggren, Synth. Met. **150**, 217 (2005).
[31] J. X. Geng and T. Y. Zeng, J. Am. Chem. Soc. **128**, 16827 (2006).
[32] L. H. Nguyen, H. Hoppe, T. Erb, S. Gunes, G. Gobsch, and N. S. Sariciftci, Adv. Funct. Mater. **17**, 1071 (2007).